



Lightning Activity Variability with Prevailing Weather Parameters and Aerosol Loading Over Dry and Wet Regions of India

M. I. R. TINMAKER,¹ ARUN K. DWIVEDI,² SAHIDUL ISLAM,² SACHIN D. GHUDE,¹ S. H. KULKARNI,² MANOJ KHARE,² and D. M. CHATE²

Abstract—This paper presents the lightning activity, aerosol optical depth (AOD) and climatic parameters (Bowen ratio, relative humidity, rainfall, maximum surface temperature and maximum updraft speed) over wet (Northeast India—NEI) and dry (Northwest India—NWI) land surfaces in a comparative analysis. The analyses are performed on flash counts and weather data of 17 years (1998–2014) retrieved from the Tropical Rainfall Measuring Mission (TRMM) lightning imaging sensors (LIS) and the Moderate Resolution Imaging Spectroradiometer (MODIS), respectively. The first higher peak for flash counts during pre-monsoon (April–May) and second lower peak during September over wet NEI and dry NWI regions indicate the development of strong electrified storms during pre-monsoon and weakly electrified clouds during the withdrawal phase of the southwest summer monsoon. The monthly means of flash counts, Bowen ratio, maximum surface temperature, AOD and maximum updraft speed are higher by 27, 81, 16, 50 and 16%, respectively, for NWI than those of NEI. The relative humidity and rainfall are higher by 12% and 73% for NEI than those of NWI, respectively. The Pearson's correlation coefficients of lightning activity with climatic parameters and AOD demonstrate the distinctive orographic lifting, moisture content and vertical wind shear in the upper troposphere in the regional climatic zone of dry NWI in comparison to that of wet NEI.

Keywords: Lightning, rainfall, Bowen ratio, maximum surface temperature, AOD.

1. Introduction

Lightning flash counts show on an average 78% of the global lightning activity in the tropical belt (30° S and 30° N) of Southeast Asia, Africa and South America regions (Cecil et al., 2014; Price, 2008;

Turman & Edgar, 1982; Williams & Satori, 2004). The relationship of lightning activity with different weather parameters shows seasonal variations in severity of convective storms from region to region (Chate et al., 2017; Tinmaker et al., 2015; Williams, 1985). In tropical regions, lightning and associated rainfall increase drastically with moisture content and deep convection in which vertical air motion plays a pivotal role in the development of thunderstorms (Chate et al., 2017; Manohar & Kesarkar, 2003; Tinmaker & Ali, 2012; Tinmaker et al., 2017). The Bowen ratio (sensible heat flux to latent heat flux ratio) is a climatic indicator of lightning intensity over oceanic and continental regions (Brooks, 2013; Brooks et al., 2003; Chate et al., 2017; Romps et al., 2014; Tinmaker et al., 2017, 2019; Toumi & Qie, 2004). Lightning flash frequency is associated with the instability in the troposphere (Radler et al., 2019). The atmospheric instability for different regions is a function of topography and weather-driven climatology through net solar radiation fluxes on seasonal scales. The convective available potential energy (CAPE) is an important ingredient for the development of seasonal clouds over different regions. It is a measure of the maximum kinetic energy required for lifting the air parcel adiabatically from the lowest layer to the upper tropospheric layer (Brooks, 2013; Romps et al., 2014). Higher CAPE leads to the maximum updraft speed for charge separations in thunderclouds which causes more lightning discharges (Williams & Stanfill, 2002). The relation between maximum updraft speed and CAPE is $W_{\max} = \sqrt{2 \times \text{CAPE}}$ (Tinmaker et al., 2017, 2019; Westermayer et al., 2016; Williams & Stanfill, 2002). Pickering et al. (1998) found that lightning frequency

¹ Indian Institute of Tropical Meteorology, Pune 411008, India.

² Centre for Development of Advanced Computing, Pune 411008, India. E-mail: chatetilip@gmail.com

is a function of maximum updraft speed in thunderstorm clouds. Barthe and Barth (2008) suggested use of maximum updraft speed for estimating the lightning initiation capability of clouds. The aerosol optical depth (AOD) is a measure of the hygroscopic aerosol concentration for the cloud condensation nuclei (CCN) as a function of relative humidity (Chate et al., 2017; Grandey et al., 2013; Jin & Wang, 2018; Tao et al., 2012; Tinmaker et al., 2017; Wang et al., 2011). Lightning involves complex interactions between atmospheric and in-cloud processes; therefore, research into that phenomenon continues to motivate researchers in this field. A large body of publications from different geographical regions demonstrates strong dependence of lightning activity on the size of storms as a function of regional climatic zones, land use/land cover (LULC) and orography of terrains. The relationships of lightning activity with the various atmospheric weather parameters and aerosol loading using long-term data are not reported for regional climatic zones of different LULC and topography in a comparative analysis. For instance, wet (Northeast India—NEI) and dry (Northwest India—NWI) are two regional climatic zones of different LULC and topography.

This work analyses the flash count and weather data of 17 years (1998–2014) retrieved from the Tropical Rainfall Measuring Mission (TRMM) lightning imaging sensors (LIS) and the Moderate Resolution Imaging Spectroradiometer (MODIS), respectively, for wet (NEI) and dry (NWI) regions. The retrieved Bowen ratio, maximum surface temperature, maximum updraft speed, relative humidity, rainfall, lightning flash counts and AOD data provide storm characteristics in wet (NEI) and dry (NWI) regional climatic zones. The paper discusses the variability of lightning activity changes as a function of Bowen ratio, relative humidity, rainfall, maximum surface temperature, maximum updraft speed and AOD for wet (NEI) and dry (NWI) regions. Also, Pearson's correlation coefficients of lightning flash counts with the weather parameters and aerosol loading support the variability of lightning activities in the wet (NEI) and dry (NWI) regions on seasonal scales.

2. Domain of the Study

The study domain of different topographical regions is shown in Fig. 1. The Northwest Indian (NWI, a dry land) region (22° N–37° N, 72° E–84° E) includes the Thar Desert which lies leeward of the Aravalli Mountains, and thus NWI experiences minimum rainfall. The Thar Desert is a large arid region in NWI. The Northeast Indian (NEI, a wet land) region (22° N–30° N and 87° E–98° E) is surrounded by the Himalaya in the north, the Meghalaya plateau in the south and the hills of Nagaland, Mizoram and Manipur in the east. NEI experiences higher frequency of lightning activity (Chakrabarty et al., 2007; Guha & De, 2009; Ghosh et al., 2008; Ray, 2000; Tinmaker & Ali, 2012). For the NEI region, 80% of annual rainfall is linked to the lightning activity with annual thunderstorm frequency of 80 days (Desai, 1950; Dikshit & Dikshit, 2014; IMD, 1944; Kalita & Sarma, 2000; Rao et al., 1971; Tinmaker & Ali, 2012).

3. Data and Methodology

The TRMM-LIS's gridded (0.5° × 0.5°—55 km × 55 km) monthly lightning flash count data set for a period of 17 years (1998–2014) was

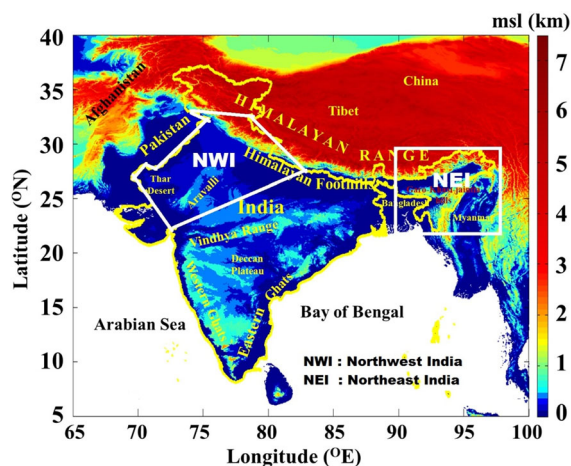


Figure 1
The study regions of Northwest India (NWI) and Northeast India (NEI)

retrieved from the NASA GHRC website (<https://lightning.nsstc.nasa.gov/nlisib/nlisearch.html>) over the NWI region (22° N–37° N, 72° E–84° E) and NEI (22° N–30° N and 87° E–98° E) region (Christian et al., 1999; Boccippio et al., 2002; Schumacher et al., 2004; Cecil et al., 2014; Chate et al., 2017; Tinmaker et al., 2015, 2017, 2019). The data sets of rainfall, relative humidity, AOD and Bowen ratio were obtained from the MODIS website (<https://disc.sci.gsfc.nasa.gov/giovanni/>). The maximum surface temperature data were fetched from the ftp server of the Indian Institute of Tropical Meteorology (<ftp://www.tropmet.res.in/pub/data/txtn/new-txregion.txt>). The CAPE data over NWI and NEI were downloaded from the University of Wyoming's website (<https://www.weather.uwyo.edu/upperair/sounding.html/>). The maximum updraft speeds were estimated from $W_{\max} = \sqrt{2 \times \text{CAPE}}$ (Williams & Stanfill, 2002). The data analyses were carried out for the pre-monsoon (March–May), monsoon (June–September), post-monsoon (October–November) and winter (December–February) over the period of 17 years (1998–2014).

Karl Pearson's measure of intensity of the linear relationship between variables (series) x and y denoted by $r(x, y)$ or r or R is referred to as Pearson's correlation coefficient. If (x_i, y_i) , $i = 1, 2, 3, \dots, n$ (n pairs of observations on variable x and y), where \bar{x} and \bar{y} are the mean of x and y variables, then the Pearson's coefficient can be expressed as:

$$r = \frac{\frac{1}{n} \sum_{i=1}^n (x_i - \bar{x})(y_i - \bar{y})}{\sqrt{\frac{1}{n} \sum_{i=1}^n (x_i - \bar{x})^2} \sqrt{\frac{1}{n} \sum_{i=1}^n (y_i - \bar{y})^2}}$$

The value of r always lies between $+1$ and -1 . If the value of r is greater than 0 (positive correlation), as the value of one variable increases, so does the value of the other variable, while if r is less than 0 (negative correlation), as the value of one variable increases, the other variable decreases. The values of r of between -0.1 and -0.3 , -0.3 and -0.5 , and -0.5 and -1.0 indicate weak, moderate and strong negative correlation coefficients, respectively. On the other hand, the values of r between 0.1 and 0.3 , 0.3 and 0.5 , and 0.5 and 1.0 refer to weak, moderate and

strong positive correlation coefficients, respectively. For examining the existence of Pearson's correlation coefficient linear relationship between two variables, the Z test expression is as below:

$$Z = \frac{(\bar{x}_1 - \bar{x}_2) - (\mu_1 - \mu_2)}{\sqrt{\left(\frac{\sigma_1^2}{n_1} + \frac{\sigma_2^2}{n_2}\right)}}$$

where μ_1 and μ_2 are hypothesized difference between the population of variables, σ_1 and σ_2 are the standard deviations of the two variables, and n_1 and n_2 are the number of observations.

4. Results and Discussion

Figures 2 and 3 show the monthly mean variation of flash count, Bowen ratio, maximum surface temperature and AOD over the period of 17 years (1998–2014) for wet NEI and dry NWI regions. It is seen from the Figs. 2 and 3 that the flash count, Bowen ratio and maximum surface temperature show their first higher peaks during pre-monsoon (April–May) and that of AOD in July over NEI and NWI regions, respectively. The monthly mean of flash counts, Bowen ratio, maximum surface temperature and AOD are found to be 27%, 81%, 16% and 50% greater for the NWI region than those of the NEI region, respectively (Fig. 2). Figures 2 and 3 shows averaged flash counts higher for the dry NWI region than that of the wet NEI region, while averaged rainfall is higher for the wet NEI region than that of the dry NWI region (Figs. 4, 5). The Bowen ratio is found to be greater than 10 for the dry (NWI) region, whereas it is less than 2 for the wet NEI region (Neog et al., 2005; Shakeel et al., 2012). The results can be attributed to the greater amount of heat released from the surface to the atmosphere in the NWI region than that of the NEI region. This is because of the higher surface temperature in the NWI region than in the NEI region. The warm moist air advection during pre-monsoon season increases the lapse rate and conditional instability for developments of severe thunderstorm with high lightning activity over the NEI region (Ghosh et al., 2008; Tinmaker & Ali, 2012). Figure 3 shows the peak lightning activity during May was associated with induced lows over

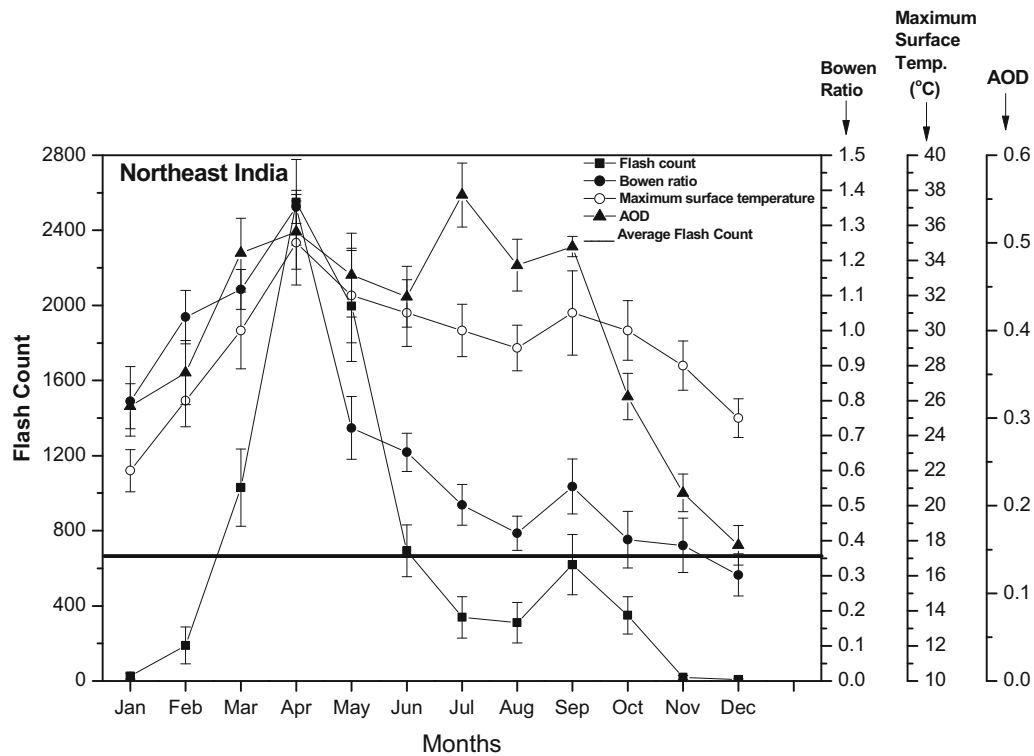


Figure 2

Monthly mean variation of flash count, Bowen ratio, maximum surface temperature and AOD over NEI for a 17-year period (1998–2014)

NWI (IMD, 1973). Figures 4 and 5 show the monthly mean variation of flash count, maximum updraft speed, relative humidity and rainfall for the period of 17 years (1998–2014) over NEI and NWI regions, respectively. Also, Figs. 4 and 5 show the first higher peaks for flash count and maximum updraft speed during pre-monsoon (April–May), while for relative humidity and rainfall, peaks appear in July over NEI and NWI regions. The first higher peak for flash count during pre-monsoon may be attributed to orography of the terrain, supply of moisture from the neighbouring Arabian Sea of the NWI region and the Bay of Bengal of the NEI region, high aerosol loading, maximum updraft speed, deep convection and strong electrical charge centres, leading to more lightning activity. All these factors play an important role in the strong electrification process and hence high lightning activity over NEI and NWI as evident in publications from different geographical regions (Middey & Kaware, 2016; Saunders et al., 1991; Yuan & Qie, 2008) that demonstrate the strong

dependence of lightning activity on the size of thunderstorm. The second lower peak of flash counts during September over NEI and NWI regions can be linked with the lower AOD owing to washout, lower cloud top, minimum updraft speed, weak electrification and hence lesser lightning activity.

Figures 4 and 5 show maximum updraft speed 16% greater over NWI than that over NEI, while relative humidity and rainfall are 12% and 73% higher, respectively, over NEI than over NWI. The higher relative humidity leads to more concentrations of cloud droplets, and maximum updraft speed results in ice particle accumulations in the cloud top region (Soula, 2009). The main charging region in a thunderstorm locates where temperature ranges from -15° to -25° °C. The efficiency of the charge separation mainly depends on relative humidity, temperature and cloud particle distribution in the storm. The larger the charge separation, the higher the electrical potential field difference that causes strong cloud electrification and subsequent lightning

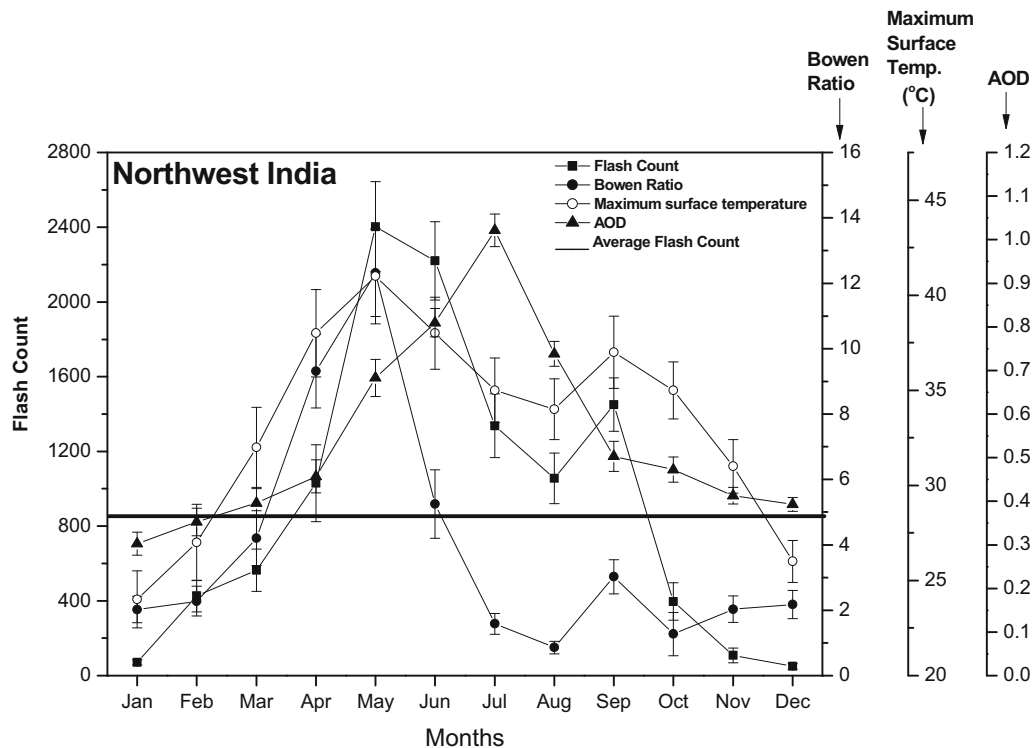


Figure 3

Monthly mean variation of flash count, maximum surface temperature and AOD over NWI for a 17-year period (1998–2014)

activity (Berdeklis & List, 2001; Houze, 2014; Khain et al., 2005; Rosenfeld et al., 2001; Shi et al., 2018; Takahashi, 1978; Williams, 1988; Williams et al., 2005). The minimum lightning flash counts observed during monsoon season with a peak in September over NEI and NWI (Figs. 4, 5) are possibly due to a lower Bowen ratio (higher latent heat flux relative to sensible heat flux). During active monsoon, less aerosol loading (AOD) owing to the washout effect, large moisture content and moderate updraft speed limits the vertical development of storms. The cloud droplets attain the size of raindrops in the storm with weak cloud electrification and hence low lightning activity (Kar & Ha, 2003; Middey & Kaware, 2016; Rosenfeld et al., 2008; Soula, 2009; Yuan & Qie, 2008).

Figure 6a–c shows the Pearson's correlations of flash count with Bowen ratio, maximum surface temperature and AOD with coefficients of $R = 0.84483$ ($R^2 = 0.71056$), $R = 0.79487$ ($R^2 = 0.62764$), and $R = 0.75029$ ($R^2 = 0.55807$),

respectively, over the NEI region. Figure 7a–c shows the Pearson's correlation of flash count with maximum updraft speed, relative humidity and rainfall with coefficients of $R = 0.66701$ ($R^2 = 0.43867$), $R = 0.70021$ ($R^2 = 0.48549$) and $R = 0.58647$ ($R^2 = 0.33444$), respectively, over the NEI region. Figure 8a–c presents the Pearson's correlations of flash counts with Bowen ratio, maximum surface temperature and AOD with coefficients of $R = 0.95159$ ($R^2 = 0.90448$), $R = 0.75354$ ($R^2 = 0.56255$) and $R = 0.69392$ ($R^2 = 0.47595$), respectively, over the NWI region. Also, Fig. 9a–c shows the Pearson's correlation of flash counts with maximum updraft speed, relative humidity and rainfall with coefficients of $R = 0.79985$ ($R^2 = 0.63562$), $R = 0.81527$ ($R^2 = 0.66081$) and $R = 0.65471$ ($R^2 = 0.42207$), respectively, over the NWI region. For both wet (NEI) and dry (NWI) regional climatic zones, the Pearson's correlation coefficients of flash counts with weather parameters show significant levels at 0.025 and a calculated z critical value of

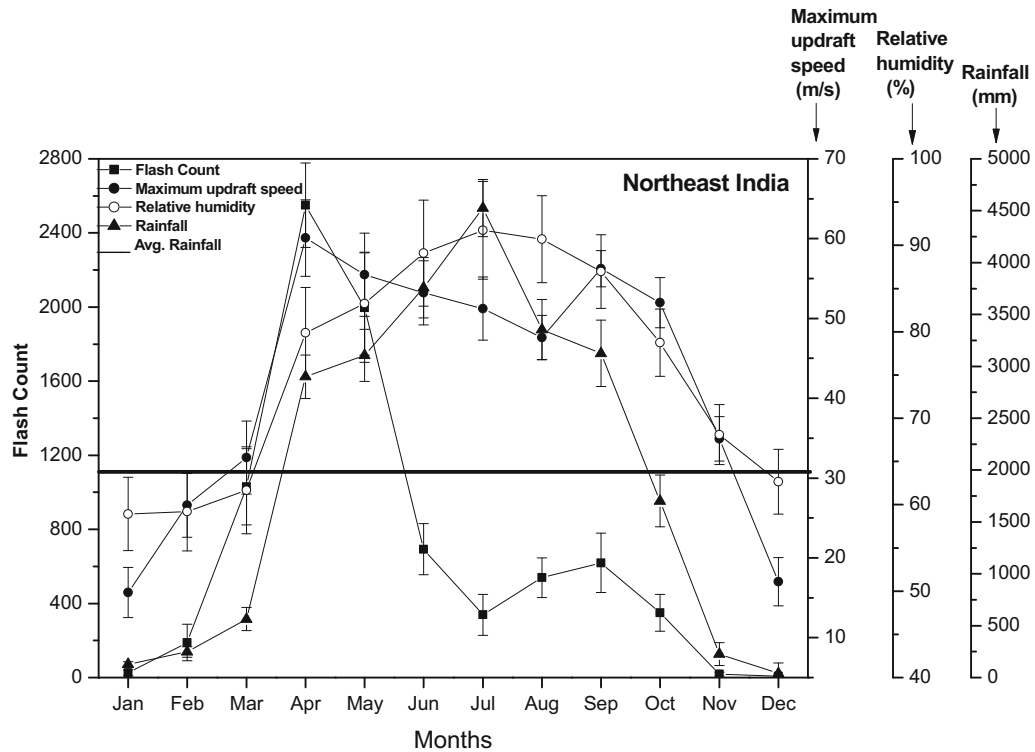


Figure 4

Monthly mean variation of flash count, maximum updraft speed, relative humidity and rainfall over NEI for a 17-year period (1998–2014)

1.96. The orographic lifting, moisture content, aerosol loading and vertical wind shear in the upper troposphere differ in the wet (NEI) and dry (NWI) regions. As a result, environmental conditions for the development of storms and their characteristics in these two regional climatic zones are entirely different (Houze Jr et al., 2007; Koteswaram & Srinivasan, 1958; Rao, 1966; Medina et al., 2010; Romatschke et al., 2010; Srinivasan et al., 1973). The cloud base in the dry (NWI) climatic zone could be around 3–4 km altitude, while the cloud base may be at ~ 1 km above ground in the wet (NEI) climatic region. Furthermore, raindrops falling below the storm in the dry (NWI) region frequently evaporate before reaching the Earth's surface, which leads to dust-storm conditions and probably contributes to aerosol loading (AOD). In summary, the storms in the wet (NEI) region are responsible for heavy rain, hail and severe squalls, while the thunderstorms in the dry

climatic region have higher lightning activity as against those in the wet climatic region.

5. Conclusions

Comparative analysis of lightning activity over climatologically different topographical regions of dry land (NWI) and wet land (NEI) as a function of Bowen ratio, relative humidity, rainfall, maximum surface temperature, updraft speed and aerosol loading (AOD) can provide an assessment of potential natural hazards over regional climatic regions of different LULC and orography. The capability of aerosol loading for CCN and convective cloud formations is also important. The major findings are summarised below.

The monthly mean variation of flash count shows that the first higher peak for flash count during pre-

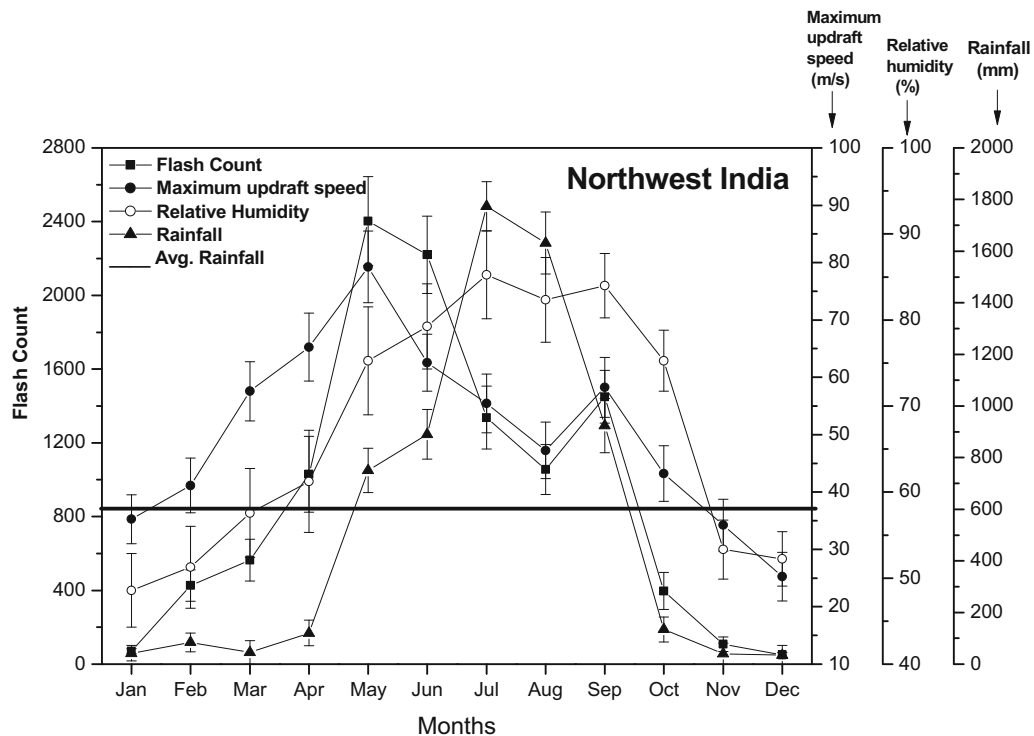


Figure 5

Monthly mean variation of flash count, maximum updraft speed; relative humidity and rainfall over NWI for a 17-year period (1998–2014)

monsoon (April–May) can be linked to the maximum surface temperature, higher Bowen ratio, aerosol loading, strong convection, maximum updraft speed and strong electrifications of thunderstorms over distinct topographical regions of wet (NEI) and dry (NWI) regions.

The second lower peak for flash count during September over wet (NEI) and dry (NWI) regions could possibly be owing to a decrease in AOD with washout during active monsoon, low cloud base height, moderate updraft speed, weakly electrified storms and hence lower lightning activity.

The dry (NWI) region shows that the greater lightning activity than that of the wet (NEI) region for the analysed data of weather parameters over 17 years (1998–2014) relates to the distinct LULC and topography of these regions of different climatic characteristics.

The monthly means of flash counts, Bowen ratio, maximum surface temperature and AOD are higher by 27%, 81%, 16% and 50%, respectively, for the dry (NWI) region than those of the wet (NEI) region. The maximum updraft speed is higher by 16% for dry NWI than that of wet NEI, while relative humidity and rainfall are higher by 12% and 73%, respectively, for wet NEI than that of dry NWI.

The good Pearson's correlation coefficients evidently support the regionally distinctive orographic lifting, moisture content, aerosol loading and vertical wind shear in the upper troposphere in dry NWI and wet NEI regions. Thus, ease of development of storms and their electrifications in wet NEI and dry NWI climatic zones of different LULC and orography are uniquely distinguishable for the possible assessments of natural disasters in these regions.

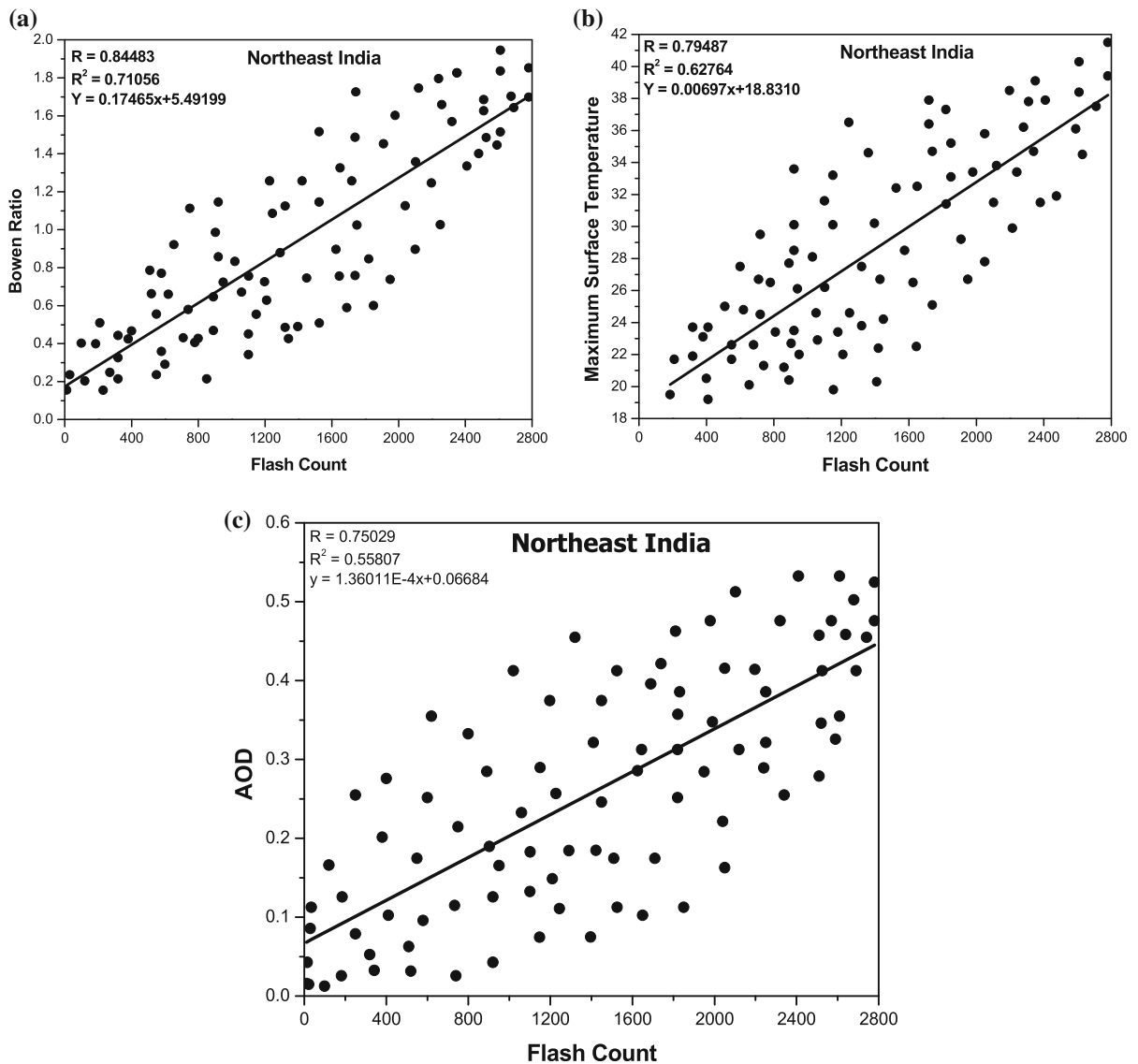


Figure 6

Correlation coefficients of flash count with **a** Bowen ratio, **b** maximum surface temperature and **c** AOD over NEI for a 17-year period (1998–2014)

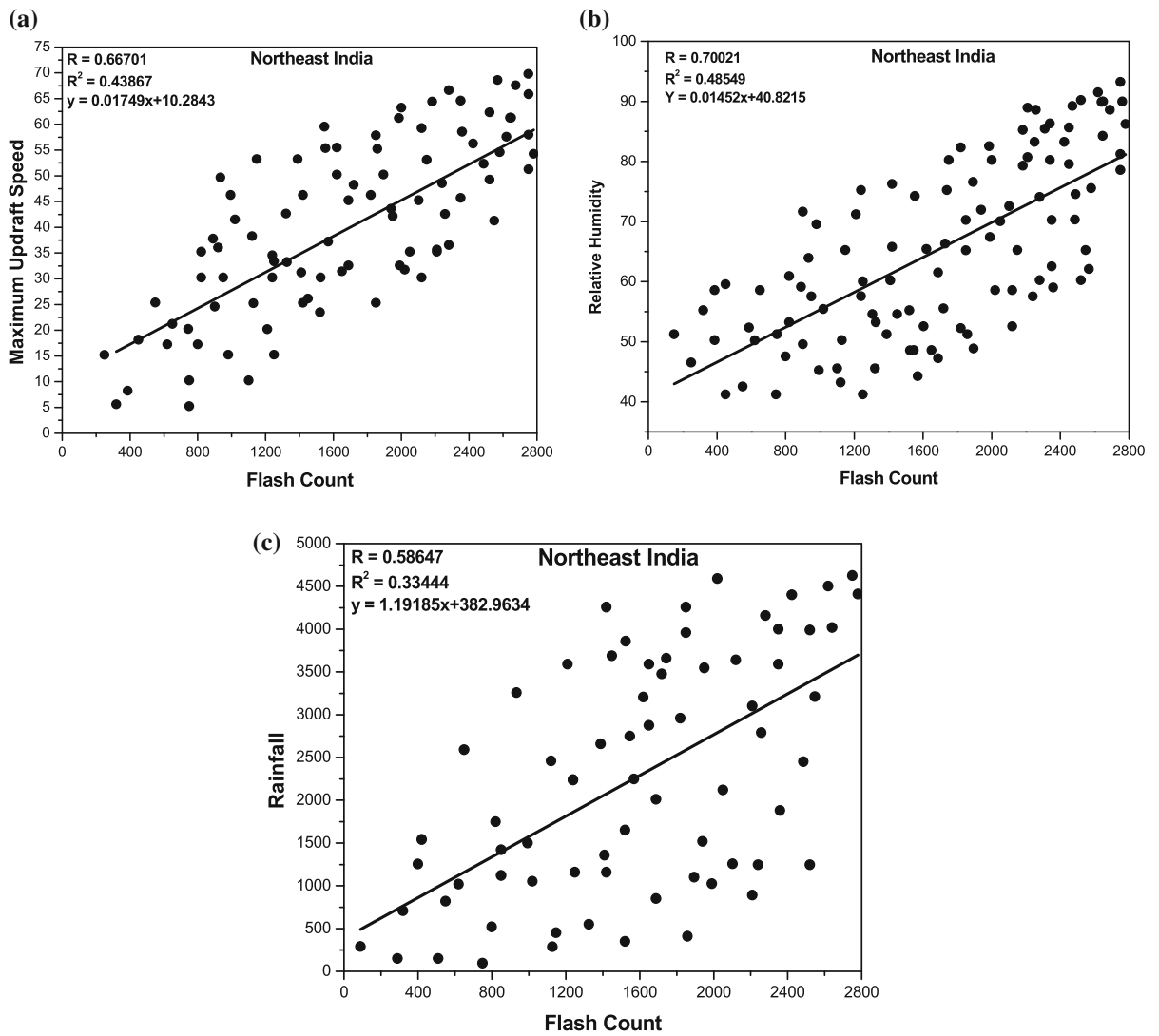


Figure 7

Correlation coefficients of flash count with **a** maximum updraft speed, **b** relative humidity and **c** rainfall over NEI for a 17-year period (1998–2014)

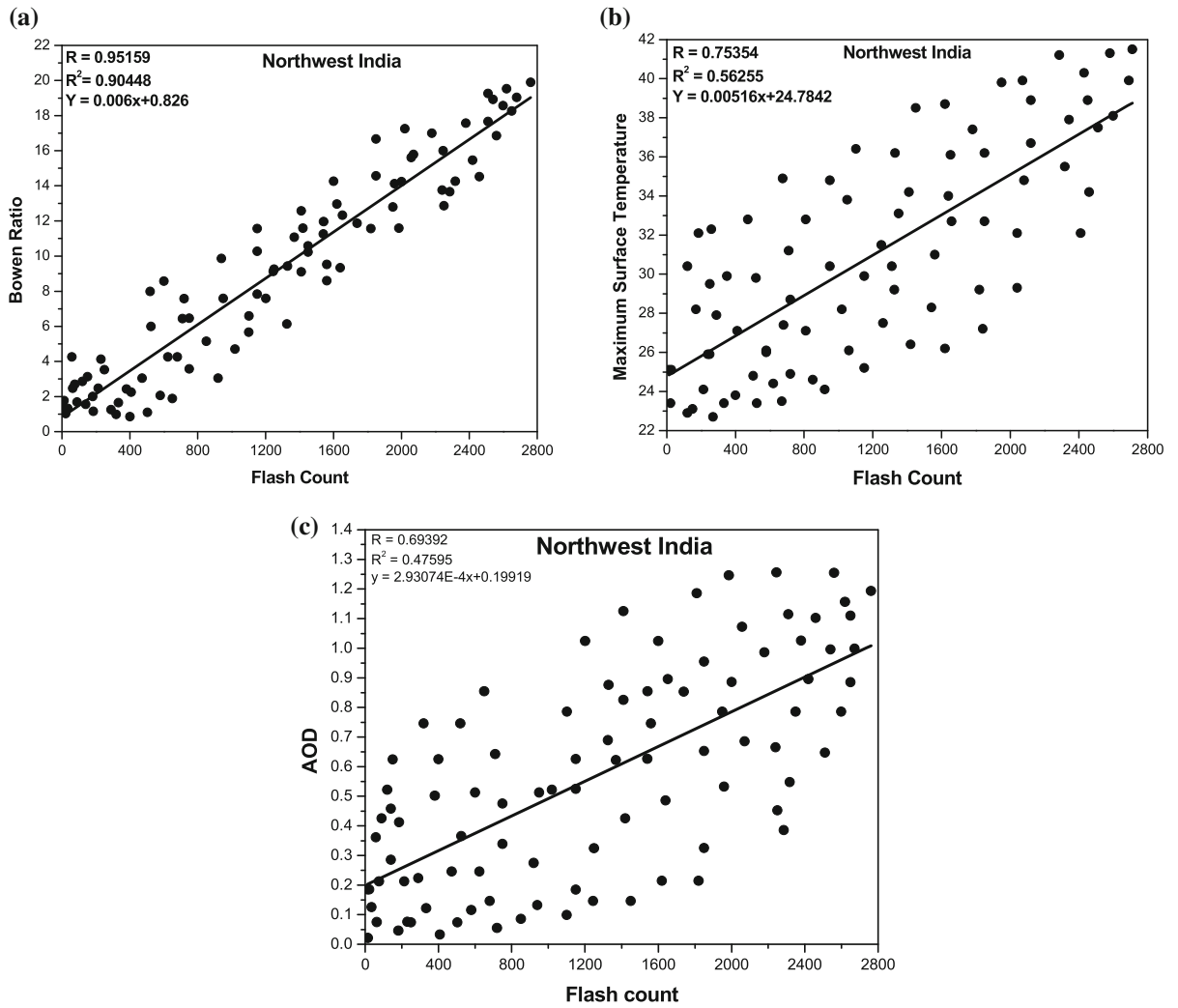


Figure 8

Correlation coefficients of flash count with **a** Bowen ratio, **b** maximum surface temperature and **c** AOD over NWI for a 17-year period (1998–2014)

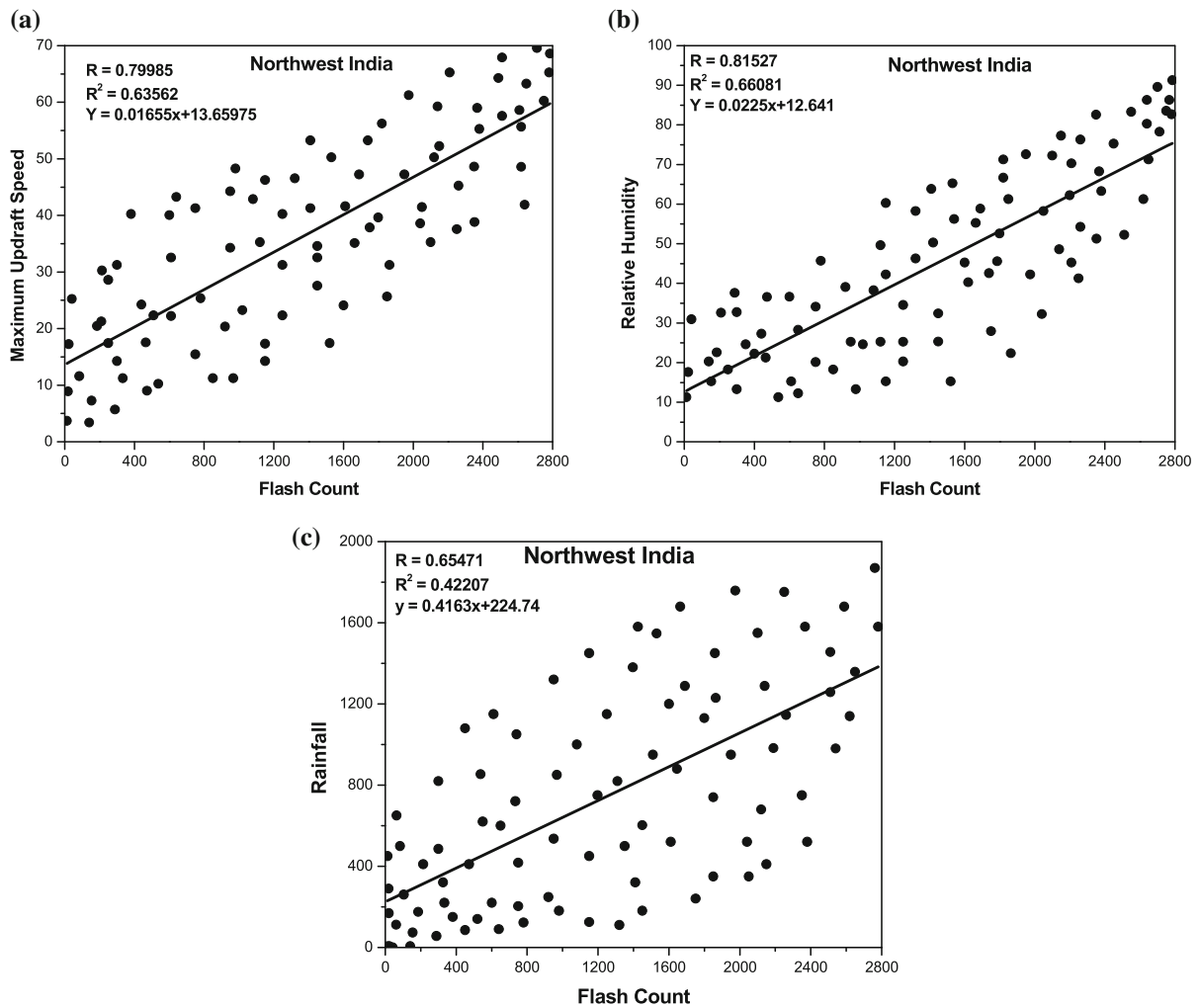


Figure 9

Correlation coefficients of **a** flash count vs maximum updraft speed, **b** flash count vs relative humidity and **c** flash count vs rainfall over NWI for a 17-year period (1998–2014)

Acknowledgements

The Ministry of Earth Sciences (Government of India) supports Indian Institute of Tropical Meteorology (IITM). Thanks to Professor R. S. Nanjundiah, Director, IITM for maximum surface temperature data (<ftp://www.tropmet.res.in/pub/data/txtn/new-txregion.txt>). The authors acknowledge the NASA GHCC for TRMM (LIS) flash count data (<http://thunder.msfc.nasa.gov/>), MODIS for sensible and latent heat fluxes, AOD, rainfall and relative humidity data (<http://disc.sci.gsfc.nasa.gov/giovanni/>) and

the University of Wyoming for CAPE data (<https://www.weather.uwyo.edu/upperair/sounding.html>).

Publisher's Note Springer Nature remains neutral with regard to jurisdictional claims in published maps and institutional affiliations.

REFERENCES

Barthe, C., & Barth, M. C. (2008). Evaluation of a new lightning-produced NO_x parameterization for cloud resolving models and

- its associated uncertainties. *Atmospheric Chemistry and Physics*, 8, 4691–4710.
- Berdeklis, P., & List, R. (2001). The ice crystal–graupel collision charging mechanism of thunderstorm electrification. *Journal of Atmospheric Sciences*, 58(18), 2751–2770.
- Boccippio, D. J., Koshak, W. J., & Blakeslee, R. J. (2002). Performance assessment of the optical transient detector and lightning imaging sensor. Part I: Predicted diurnal variability. *Journal of Atmospheric and Oceanic Technology*, 19, 1318–1332.
- Brooks, H. E. (2013). Severe thunderstorms and climate change. *Atmospheric Research*, 123, 129–138.
- Brooks, H. E., Lee, J. W., & Craven, J. P. (2003). The spatial distribution of severe thunderstorm and tornado environments from global reanalysis data. *Atmospheric Research*, 67, 73–94.
- Cecil, D. J., Buechler, D. E., & Blakeslee, R. J. (2014). Gridded lightning climatology from TRMM LIS and OTD: Dataset description. *Atmospheric Research*, 135, 404–414.
- Chakrabaty, K. K., Nath, A. K., & Sengupta, S. (2007). Nor'wester over west Bengal and comfortability. *Mausam*, 58, 177–188.
- Chate, D. M., Tinmaker, M. I. R., Aslam, M. Y., & Ghude, S. D. (2017). Climate indicators for lightning over sea, sea–land mixed and land-only surfaces in India. *International Journal of Climatology*, 37, 1672–1679.
- Christian, H. J., Blakeslee, R. J., Goodman, S. V., Mach, D. A., Stewart, M. F., Buechler D. E., et al. (1999). The lightning imaging sensor. In *Proceeding of 11th international conference on Atmospheric Electricity National Aeronaut and Space Administration*, AI, pp. 746–749.
- Desai, B. N. (1950). Mechanism of Nor'wester of Bengal. *Indian Journal of Meteorology and Geophysics*, 1, 74–76.
- Dikshit, K. R., & Dikshit, J. K. (2014). *Weather and climate of north-east India*. In *North-east India: Land, people and economy* (pp. 149–173). Springer.
- Ghosh, A., Lohar, D., & Das, J. (2008). Initiation of nor'wester in relation to mid-upper and low-level water vapor patterns of METEOSAT-5 images. *Atmospheric Research*, 787, 116–135.
- Grandey, B. S., Stier, P., & Wagner, T. M. (2013). Investigating relationships between aerosol optical depth and cloud fraction using satellite, aerosol reanalysis and general circulation model data. *Atmospheric Chemistry and Physics*, 13, 3177–3184.
- Guha, A., & De, B. K. (2009). Lightning electrical characteristics during tropical summer thunderstorm in North-east India. *Journal of Atmospheric and Solar Terrestrial Physics*, 71, 1365–1373.
- Houze, R. A., Jr. (2014). Cumulonimbus and severe storms. *International Geophysics*, 104, 187–236.
- Houze, R. A., Jr., Wilton, D. C., & Smull, B. F. (2007). Monsoon convection in the Himalayan region as seen by the TRMM precipitation radar. *Quarterly Journal of Royal Meteorological Society*, 133, 1389–1411.
- India Meteorological Department (IMD). (1944). Nor'westers of Bengal. *Technical Notes*, 10, 1–30.
- India Meteorological Department (IMD). (1973). Summer–Nor'westers and Andhis and large scale convective activity over peninsula and central parts of the country. Forecasting Manual: Part-III, FMU Rep. No.III-2.2, 1–145.
- Jin, Q., & Wang, C. (2018). The greening of northwest Indian subcontinent and reduction of dust abundance resulting from Indian summer monsoon revival. *Scientific Report*, 8(4573), 1–9.
- Kalita, S., & Sarma, R. (2000). Thunderstorm activity in northeast India during premonsoon period. In *Proceeding of TROPMET-2000: Ocean and Atmosphere*, 517–522.
- Kar, S. K., & Ha, K. J. (2003). Characteristics differences of rainfall and cloud-to ground lightning activity over South Korea during the summer monsoon season. *Monthly Weather Review*, 131, 2312–2323.
- Khain, A., Rosenfeld, D., & Pokrovsky, A. (2005). Aerosol impact on the dynamics and microphysics of deep convective clouds. *Quarterly Journal of Royal Meteorological Society*, 131, 2639–2663.
- Koteswaram, P., & Srinivasan, V. (1958). Thunderstorms over Gangetic west Bengal in the premonsoon season and synoptic factors favourable of their formation. *Indian Journal of Meteorology and Geophysics*, 9, 301–312.
- Manohar, G. K., & Kesarkar, A. P. (2003). Climatology of thunderstorm activity over the Indian region: 1. A study of east-west contrast. *Mausam*, 54, 819–828.
- Medina, S., Houze, R. A., Kumar, A., & Niyogi, D. (2010). Summer monsoon convection in the Himalayan region: Terrain and land cover effects. *Quarterly Journal of Royal Meteorological Society*, 136, 593–616. <https://doi.org/10.1002/qj.601>
- Middey, A., & Kaware, P. B. (2016). Disposition of lightning activity due to pollution load during dissimilar seasons as observed from satellite and ground-based data. *Climate*, 4(28), 1–12.
- Neog, P., Srivastava, A. K., & Chakravarty, N. V. K. (2005). Estimation and application of Bowen ratio fluxes over crop surfaces: An overview. *Journal of Agriculture Physics*, 5(1), 36–45.
- Pickering, K. E., Wang, Y., Tao, W. K., Price, C., & Müller J. F. (1998). Vertical distribution of lightning NO_x for use in regional and global chemical transport models. *Journal of Geophysical Research: Atmosphere*, 103(D23), 31203–31216.
- Price, C. (2008). Will a drier climate result in more lightning? *Atmospheric Research*, 91, 479–484.
- Radler, A. T., Re, M., Groenemeijer, P. H., Faust, E., Sausen, R., & Pucik, T. (2019). Frequency of severe thunderstorms across Europe expected to increase in the 21st century due to rising instability. *Climate and Atmospheric Science*, 2(1), 1–5.
- Rao, K. N., Daniel, C. E. J., & Balasubramanian, L. V. (1971). Thunderstorms over India. *India Indian Meteorological Science Report*, 153, 1–22.
- Rao, K. P. R. (1966). Thunderstorm studies in India—a review. *Indian Journal of Meteorology and Geophysics*, 12, 3.
- Ray, T. K. (2000). Meteorology of northeast India beyond year 2000. In *Proceeding of TROPMET-1999*, 348–353.
- Romatschke, U., Medina, S., & Houze, R. A. Jr. (2010). Regional, seasonal, and diurnal variations of extreme convection in the south Asian region. *Journal of Climate*, 23, 419–439. <https://doi.org/10.1175/2009JCLI3140.1>
- Romps, D. M., Seeley, J. T., Vollaro, D., & Molinari, J. (2014). Projected increase in lightning strikes in the United States due to global warming. *Science*, 346(6211), 851–854.
- Rosenfeld, D., Lohmann, U., Raga, G. B., O'Dowd, C. D., Kulmala, M., Guzzi, S., Reissell, A., & Andreae, M. O. (2008). Flood or drought: How do aerosols affect precipitation? *Science*, 321, 1309–1313.
- Rosenfeld, D., Rudich, Y., & Lahav, R. (2001). Desert dust suppressing precipitation: A possible desertification feedback loop.

- Proceeding of the National Academy of Sciences*, 98(11), 5975–5980.
- Saunders, C. P. R., Keith, W. D., & Mitzeva, R. P. (1991). The effect of liquid water on thunderstorm charging. *Journal of Atmospheric Research: Atmosphere*, 96(D6), 11007–11017.
- Schumacher, C., Houze, R. A., Jr., & Kraucunas, I. (2004). The tropical dynamical response to latent heating estimates derived from the TRMM precipitation radar. *Journal of Atmospheric Sciences*, 61, 1341–1358.
- Shakeel, A., Dobler, A., & Bodo, A. (2012). Soil moisture-precipitation feedback processes in the Indian summer monsoon season. *Journal of Hydrology*, 13(5), 1461–1474.
- Shi, Z., Tan, Y., Liu, L., Liu, J., Lin, X., Wang, M., & Luan, J. (2018). Effects of relative humidity on electrification and lightning discharges in thunderstorms. *Terrestrial Atmospheric and Oceanic Science*, 29(6), 695–708.
- Soula, S. (2009). Lightning and precipitation: Chapter 20, Lightning: Principles, instruments and applications. In H. D. Betz, U. Schumann, P. Laroche (Eds.), University of Florida Lightning Research Group. ISBN: 978-1-4020-9078-3, pp. 447–463.
- Srinivasan, V. K., Ramamuthy, Y. R., & Nene, Y. R. (1973). Summer–Nor’westers and Andhis and large scale convective activity over peninsula and central parts of the country. India Meteorological Department, Forecasting Manual Part III. p. 73.
- Takahashi, T. (1978). Riming electrification as a charge generation mechanism in thunderstorms. *Journal of Atmospheric Sciences*, 35(8), 1536–1548.
- Tao, W. K., Chen, J. P., Li, Z., Wang, C., & Zhang, C. D. (2012). Impact of aerosols on convective clouds and precipitation. *Reviews of Geophysics*, 30(RG2001), 6472–6488.
- Tinmaker, M. I. R., & Ali, K. (2012). Space time variation of lightning activity over northeast India. *Meteorologische Zeitschrift*, 21(2), 135–143.
- Tinmaker, M. I. R., Aslam, M. Y., & Chate, D. M. (2015). Lightning activity and its association with rainfall and convective available potential energy over Maharashtra, India. *Natural Hazards*, 77, 293–304.
- Tinmaker, M. I. R., Aslam, M. Y., Ghude, S. D., & Chate, D. M. (2017). Lightning with rainfall during El Nino and La Nina events over India. *Theoretical and Applied Climatology*, 130, 391–400.
- Tinmaker, M. I. R., Ghude, S. D., & Chate, D. M. (2019). Land–sea contrasts for climatic lightning activity over Indian region. *Theoretical and Applied Climatology*, 138, 931–940.
- Toumi, R., & Qie, X. (2004). Seasonal variation of lightning on the Tibetan Plateau: A spring anomaly? *Geophysical Research Letters*, 31(L04115), 1–4.
- Turman, B. N., & Edgar, B. C. (1982). Global lightning distributions at dawn and dusk. *Journal of Geophysical Research: Atmosphere*, 87, 1191–1206.
- Wang, M., Ghan, S., Ovchinnikov, M., Liu, X., Easter, R., Kasianov, E., Qian, Y., & Morrison, H. (2011). Aerosol indirect effects in a multi-scale aerosol-climate model PNNL-MMF. *Atmospheric Chemistry and Physics*, 11, 5431–5455.
- Westermayer, A. T., Groenemeijerl, P., Pistotnik, G., Sausen, R., & Eberhard, F. (2016). Identification of favorable environments for thunderstorms in reanalysis data. *Meteorologische Zeitschrift*, 26, 5431–5455.
- Williams, E. R. (1985). Large-scale charge separation in thunderclouds. *Journal of Geophysical Research: Atmosphere*, 90, 6013–6025.
- Williams, E. R. (1988). Charge separation: The electrification of thunderstorms. *Scientific American*, 259(5), 88–99.
- Williams, E. R., & Satori, G. (2004). Lightning, thermodynamic and hydrological comparison of the two tropical continental chimneys. *Journal of Atmospheric and Solar Terrestrial Physics*, 66, 1213–1231.
- Williams, E. R., & Stanfill, S. (2002). The physical origin of the land–ocean contrast in lightning activity. *Comptes Rendus Physique*, 3(10), 1277–1292.
- Williams, E. R., Mustak, V., Rosenfeld, D., Goodman S. V., & Boccippio, D. J. (2005). Thermodynamic conditions favorable to superlative thunderstorm updraft, mixed phase microphysics and lightning flash rate. *Atmospheric Research*, 76, 288–306.
- Yuan, T., & Qie, X. (2008). Study on lightning activity and precipitation characteristics before and after the onset of the South China Sea summer monsoon. *Journal of Geophysical Research: Atmosphere*, 113(D14101), 1–10.